

Influence of *Proteus spp.* on Trimethylamine N- Oxide production via the Choline Metabolism Pathway and the Formulation of a Predictive Model to Assess the Risk of Coronary Artery Disease in Indian Patients

Karan Ramu¹, Adarsh V¹, Ananya Rajagopal¹, Reeta Varyani², Prayaag Kini², Prakash Kumar², Sasmita Sabat^{1*}

1. Department of Biotechnology, PES University, Banashankari, Bangalore, Karnataka, India
2. Department of Cardiology, Sri Sathya Sai Institute of Higher Medical Sciences, EPIP Area, Whitefield, Bangalore, Karnataka, India

ABSTRACT

Background and Aim: *Proteus* bacteria, a key contributor to several gastrointestinal diseases, is known to survive in the wide pH range offered by different locations of the GI tract. The bacterial enzyme Choline TMA Lyase found in several opportunistic gut commensals catalyzes choline conversion to trimethylamine, a precursor of the pro-atherosclerotic metabolite trimethylamine N oxide. This study evaluates the pathogenic potential of *Proteus* gut bacteria in patients with coronary artery disease. We also sought to create a simple predictive model for assessing risk factors of coronary artery disease using a sample of Indian patients.

Materials and Methods: The study included 14 patients with coronary artery disease and 6 controls. Optimal conditions were devised, and standardized protocols were followed to culture *Proteus* bacteria in vitro and isolate the protein of interest, Choline TMA Lyase. FTIR analysis and UV spectrophotometry were employed to quantify choline and trimethylamine N oxide levels, respectively. Finally, receiver operating characteristic analysis and multivariate logistic regression established the predictive power of the entire model and trimethylamine N oxide.

Results: The findings demonstrated an optimum activity of this protein and the bacterial growth in the pH range of 7.4 - 9. Quantitative analysis showed trimethylamine N oxide levels to be significantly higher in coronary artery disease patients (1.81 μ M) than in controls (0.86 μ M).

Conclusion: Optimum activity in the alkaline condition indicates the strong pathological potential of *Proteus* bacteria in the progression of coronary artery disease. The prediction model can serve as a helpful tool within the medical community to assess the risk factors for coronary artery disease.

Keywords: Choline TMA-Lyase, Coronary artery disease, FTIR spectroscopy, *Proteus*, ROC curve

Received: 2021/08/26;

Accepted: 2022/01/30;

Published Online: 2022/03/20

Corresponding Information:

Sasmita Sabat, Department of Biotechnology, PES University, Banashankari, Bangalore, Karnataka, India

Email: sasmitasabat@pes.edu



Copyright © 2021, This is an original open-access article distributed under the terms of the Creative Commons Attribution-noncommercial 4.0 International License which permits copy and redistribution of the material just in noncommercial usages with proper citation.

Use your device to scan and read the article online



Ramu K, V A, Rajagopal A, Varyani R, Kini P, Kumar P et al. Influence of *Proteus spp.* on Trimethylamine N- Oxide production via the Choline Metabolism Pathway and the Formulation of a Predictive Model to Assess the Risk of Coronary Artery Disease in Indian Patients. Iran. Iran J Med Microbiol. 2022; 16 (3) :233-243

Download citation: [BibTeX](#) | [RIS](#) | [EndNote](#) | [Medlars](#) | [ProCite](#) | [Reference Manager](#) | [RefWorks](#)

Send citation to: [Mendeley](#) | [Zotero](#) | [RefWorks](#)

1 Introduction

Over the past decade, it has been proved that gut microbiota plays a vital role in human metabolism, immunity, and reactions to diseases. Dynamic elements including diet, age, sex, and ethnicity can affect the gut microbiome (1). Recent research of the gut microbiome has moved towards identifying its relationship with metabolic diseases like coronary artery disease (CAD). Choline, trimethylamine N-oxide (TMAO), and betaine, three metabolic by-products of

the bacteria, have been identified to develop risks of CAD. The metabolic pathway linking microbiota metabolism of dietary choline to CAD pathogenesis in humans has been reported elsewhere (2,3). TMAO has been shown to be pro-atherogenic and induce cardiovascular risks (4,5).

The all-important protein for choline-derived TMA formation in the gut is present only in selected bact-

eria. Interestingly, the bacteria which harbor this protein are present in small numbers in the gut of a healthy individual. Of these bacteria, the *Proteus* genus, motile Gram-negative bacterium (6), a known pathogen implicated in Crohn's disease and urinary tract infections (7), has been identified to possess the *cutC* gene, which encodes for choline TMA lyase. Other pathogenic gut bacterial groups like *Klebsiella spp.*, *Clostridium spp.*, *Desulfovibrio spp.*, and *Escherichia coli* also possess this *cutC* gene. It is plausible that these bacteria may exert singular and synergistic dysbiotic effects towards CAD progression. In this study, we set out to evaluate the pathogenic potential of the *Proteus* genus as a first step to identify key players in the gut microbiome which influence CAD.

Several properties of *Proteus* point towards its pathogenic potential in the human gut. Firstly, this genus is characterized by its swarming capability; it can transform and produce flagella-assisted motile cells (8), accentuated under anaerobic choline metabolism conditions (7-9). Secondly, fimbriae and adhesions contribute to adhesion to epithelial surfaces, leading to biofilms (10). Thirdly, the gut of typical healthy human individuals is colonized by various combinations of *Proteus vulgaris*, *Proteus mirabilis*, and *Proteus penneri*, which together comprise less than 0.05% of the entire diverse gut microbiota (11). Fourthly, *Proteus* bacteria are known to survive in a wide pH range of 2-10, conferring a survival advantage in all the compartments of the GI tract.

Taken together, this strongly suggests that *Proteus* bacteria is a key member of the dysbiotic state of the gut microbiome. Specifically, it may be inferred that an increase in the proportion of pathogenic gut bacteria (particularly the *Proteus* genus), when additionally compounded by the presence of favorable conditions of pH and metabolites like choline, could contribute to the exacerbation of dysbiosis.

In the current study, we investigated the pathogenic potential of *Proteus* bacteria in CAD progression, using *P. mirabilis* and *P. vulgaris* as two representative organisms. Additionally, we sought to create a prediction model to diagnose CAD in an Indian cohort of CAD patients. Through an *in silico* study on choline TMA lyase in *P. vulgaris*, a pH range of 7 to 8.5 was identified to be optimal for this protein's functionality. Taking this study of Choline TMA Lyase activity forward, we developed standardized salting out and growth curves to verify an optimal pH for both choline TMA lyase activity and organism growth, respectively. Additionally, we quantified choline and TMAO levels in Indian CAD patients to devise a template for a predictive model for CAD diagnosis.

2. Materials and Methods

Sample Collection

Proteus Bacteria

P. mirabilis and *P. vulgaris* bacterial samples were collected from patients with risks of coronary artery disease at Kempegowda Institute of Medical Sciences (KIMS) Bangalore, India.

CAD Patient Serum Samples

Our study included 20 patients, 14 CAD patients (8 men, 6 women, mean age = 45.07±15.42 years old) and 6 controls (3 men, 3 women, mean age = 40.52±21.82 years old). Inclusion parameters comprised the history of diabetes, obesity, hypertension, and smoking. Details of the cohort of the patients have been summarised in [Table 2](#).

Characterization Tests

The characterization of the bacterial samples procured from KIMS was performed by gram staining, catalase test and indole test as described (12). Nutrient agar (HiMedia), nutrient broth (HiMedia) and MacConkey agar (HiMedia) were used for the cultivation of bacteria which was performed at 15psi 121.5°C for 15 min along with an incubation period of 18 h at 37°C.

For the study at different pH 2.5, 6.4, 7.4, 8.5 and 9, the medium was adjusted using sterilized 1M HCl and 1M NaOH. The prerequisite for plotting the growth curve was optimizing pH in nutrient broth (NB) (pH 7.4) to 2.5, 6.4, 7.4, 8.5 and 9, using 1M HCl and 1M NaOH, followed by autoclaving it at 15psi, 15 mins & 121.5°C. To prepare the required bacterial suspensions for our study, we followed the standard inoculum development procedure: adding a loopful of bacteria to 5ml NB (pH 7.2±0.2) and incubating at 37°C for 18 h. Further, 2.5 mL of the inoculum was added to test tubes, each containing 25 mL of pH optimized NB and stored at 37°C, with gentle shaking at 200 rpm.

The absorbance of the broth culture was measured at 600 nm (OD600) using a UV spectrophotometer (Eppendorf, India) for 8 continuous hours at 1-hour intervals. Growth curves were plotted for both species.

Ammonium Sulphate Precipitation

The partial purification of proteins using extrapure ammonium sulfate precipitation was performed with 1 mL of the incubated (18 h) crude bacterial sample (13). The ammonium sulfate concentration ranged from 30-60%.

Dialysis

Partial purification of the protein from the bacterial sample was carried out using a dialysis bag (MWCO 10kDA) (13).

Total Protein Quantification by Lowry's Method

Lowry's method estimated the total protein concentration from the 18 hours harvested culture (14). A BSA standard curve was plotted within the range of 0-1000µg/mL.

SDS-PAGE

The molecular weight of the partially purified protein was identified by SDS-PAGE (15).

Choline Estimation

The choline estimation was performed from patients' serum samples (16). A choline standard curve was plotted within the range of 0-10 µg/mL. This range was chosen after a review of several studies which had measured choline levels in CVD patients and controls (17).

Trimethylamine-N-oxide (TMAO) Estimation

The TMAO estimation was performed from patients' serum samples (18). The TMAO standard curve was plotted within the range of 0-10 µM. After reviewing several studies that measured TMAO levels in CVD patients and controls, this range was chosen.

FTIR Spectroscopy

The qualitative estimation was performed using FTIR spectroscopy from patients' serum as described (19). The infrared spectra of choline and TMAO (Sigma-Aldrich) were measured using the Perkin Elmer FTIR model 2000 spectrophotometer (PerkinElmer India Pvt Ltd). The absorption and transmittance spectrum was recorded in the wavenumber range from 4000 cm⁻¹ to 400cm⁻¹. OriginPro (version 2019b) was used for data acquisition and handling.

Predictive Model

Statistical Analysis

A receiver operator characteristics (ROC) graph was plotted to obtain a cut-off value for a model based on the selected parameters. Next, multivariate logistic regression was performed using R Studio.

3.Results

Characterization of *Proteus* Bacteria

Gram Staining

The bacteria were characterized by gram staining. Observation of bacteria from both species under 100X (oil immersion) magnification after the gram staining protocol revealed pink-colored short rod-shaped bacteria, confirming the gram-negative nature of *Proteus* bacteria.

Catalase Test

A brisk effervescence was observed immediately after the addition of H₂O₂ to both bacterial species, indicating the presence of catalase.

Indole Test

After adding the Kovac's indole reagent to the incubated test tubes, a red-colored ring and green colored ring were obtained for *P. vulgaris* and *P. mirabilis* (and control), respectively. This indicates that *P. vulgaris* bacteria contain the tryptophanase enzyme while *P. mirabilis* does not. Additionally, this serves as a distinguishing test between *P. vulgaris* and *P. mirabilis*.

The combination of tests mentioned above was sufficient to identify the isolate obtained as *Proteus* species.

Measurement of Growth Curve

As shown in Figure 1, the turbidimetric growth curves were generated using the ggplot2 package in R Studio (v1.4.1717-3) for each bacterial species based on the changes in the OD (measured at 600 nm) due to bacterial growth over time. It produces a by-subject plot of predicted growth curves with associated data values and an aggregated by-group plot of growth curves, and a smoother line for each group based on user input.

Statistical analysis on the growth curve dataset was performed by calculating the generation time and specific growth rate represented by T_d and k, respectively (Figure 2a and 2b).

This growth rate is calculated by identifying the best fit of the log phase of the curve. To produce the best fit curve, the Y-axis of the log phase data was converted into the logarithmic scale. This transforms the exponential growth curve into a straight line. Now, the OD values at the beginning and end of the log phase, X₀ and X_t, respectively, were used to calculate the growth rate using the formula

$$\text{Specific growth rate } k = \frac{\log(X_t) - \log(X_0)}{X_0 \cdot 0.301t}$$

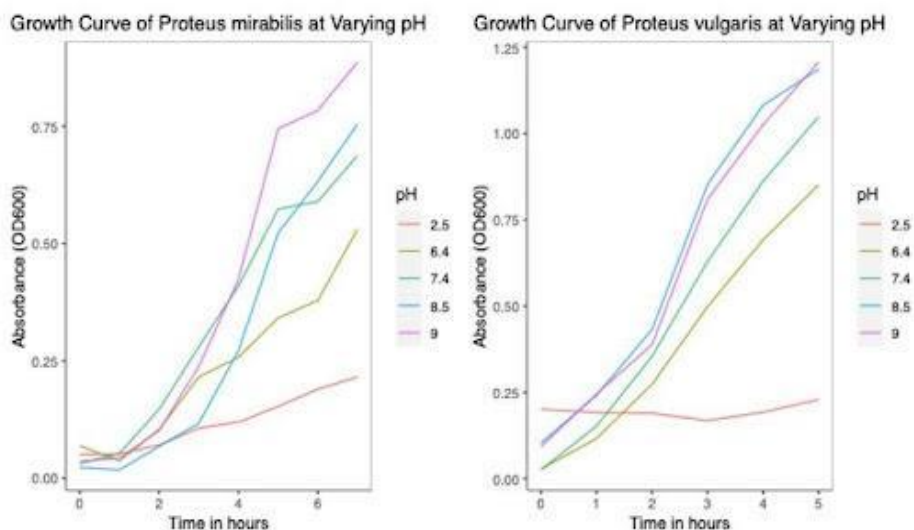


Figure 1. Growth curves of *Proteus mirabilis* (Left) and *Proteus vulgaris* (Right) at varying pH.

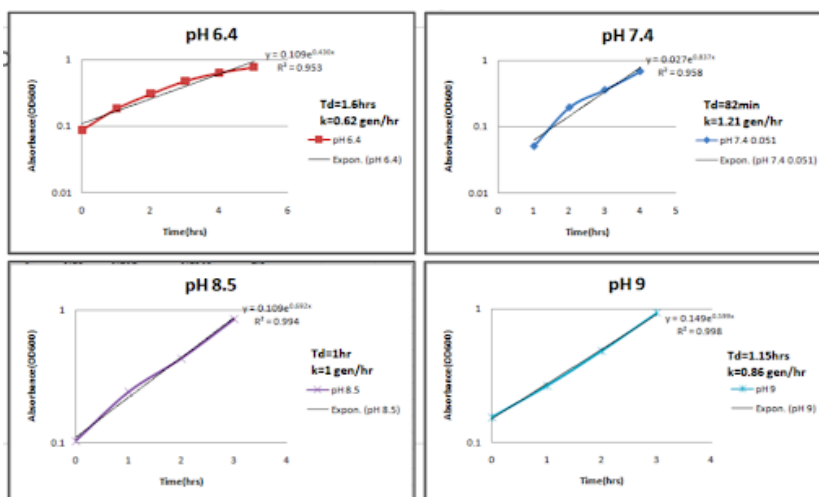


Figure 2a. Best fit curves of the log phase of the *Proteus vulgaris* growth curves.

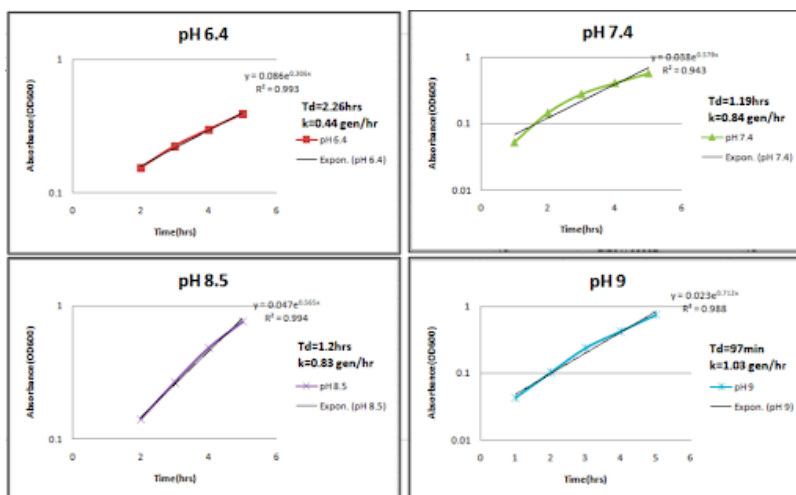


Figure 2b. Best fit curves of the log phase of the *Proteus mirabilis* growth curves.

Total Protein Estimation by Lowry's Method

The BSA standard curve was plotted at 660 nm. The unknown protein concentrations extracted and partially purified for each of the salt concentrations at all pH conditions were estimated regarding this

standard. Additionally, we plotted graphs that depicted the saturation curves of *P. vulgaris* and *P. mirabilis* at varying pH states. The total protein concentrations were plotted against the salt concentrations used for precipitation ([Figure 3](#)).

Saturation Curve of *Proteus vulgaris* at Varying pH

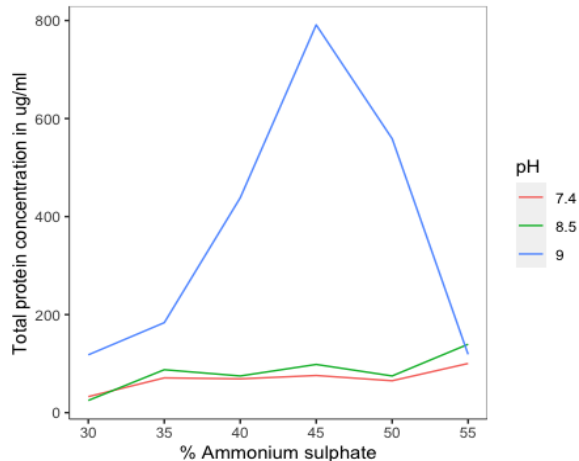


Figure 3a. Saturation curves of *Proteus vulgaris* at varying pH states.

Saturation Curve of *Proteus mirabilis* at Varying pH

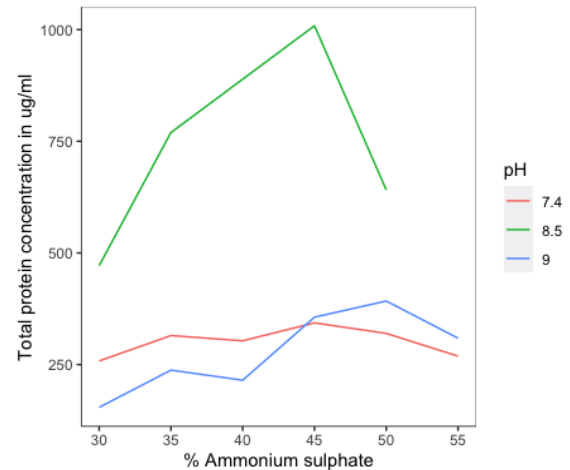


Figure 3b. Saturation curves of *Proteus mirabilis* at varying pH states.

SDS-PAGE

The gel generated by SDS-PAGE to ascertain the presence of protein fractions in each aliquot showed many bands. In particular, multiple bands were observed in the 29 - 97kDa range, and a single band

was observed between 97-200kDa ([Figure 4](#)). This sole band between 200kDa and 97kDa (present around the 120 kDa mark) in the lanes could be the protein of interest as the molecular weight of choline TMA lyase is ~124kDa ([20](#)).

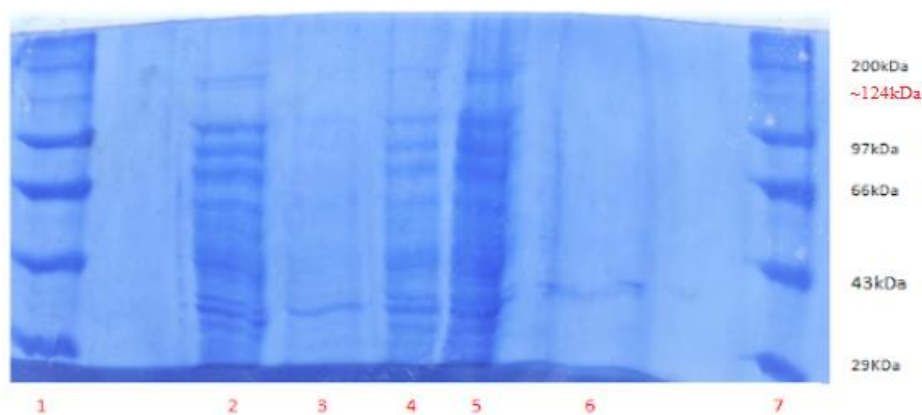


Figure 4. SDS-PAGE of the whole-cell protein. Lane 1: Protein Marker,

Lane 2: Crude 1(3μL), Lane 3: AS+D supernatant (150 μL), Lane 4: AS+D pellet (5μL), Lane 5: AS pellet (5μL),

Lane 6: AS supernatant (50 μL), Lane 7: Protein marker.

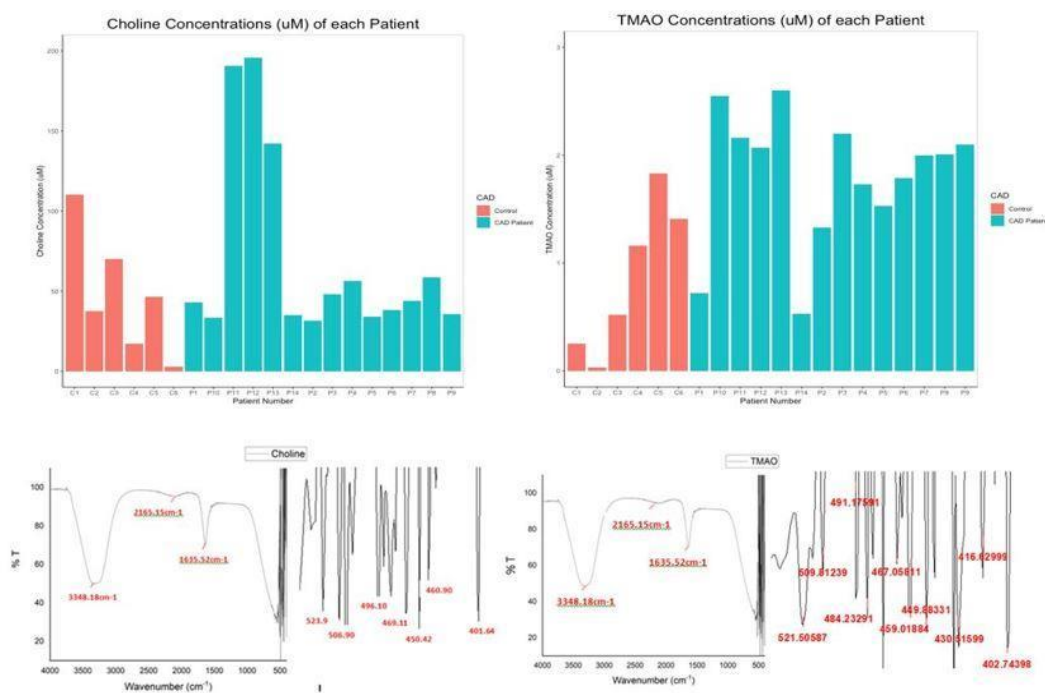


Figure 5. Top Row: Bar Plot Depicting the (a) Choline Concentrations (in μM) (b) TMAO Concentrations (in μM) of Each Individual. Bottom Row: FTIR spectrum depicting wavenumber against transmittance for standard c) choline and d) TMAO.

Choline Estimation

We identified that the choline concentration occurs within a broad range of 25 to 60 μM , in both controls and CVD patients. Using this graph as a reference, the choline concentrations in the serum samples of controls and patients using UV spectrophotometry at 365 nm were measured. Figure 5a summarizes the choline concentrations of all 20 samples analyzed in this study. The average choline concentrations in controls and CAD patients were 47.34 μM (46.35 - 48.32 μM) and 70.37 μM (69.38 - 71.36 μM), respectively, with a confidence interval of 95%.

TMAO Estimation

Figure 5b summarizes the TMAO concentrations of all 20 samples analyzed in this study. The average TMAO concentrations in controls and CAD patients are 0.86 μM (0.85 - 0.88 μM) and 1.81 μM (1.79 - 1.82 μM) respectively.

FTIR Spectroscopy

The spectra of choline and TMAO have a very strong and broad band at 3348.18 cm^{-1} , a weak peak at 2165.15 cm^{-1} and a sharp peak at 1635.52 cm^{-1} , as shown in Figures 5c and 5d. These bands characterize the functional groups present in both compounds. The distinguishing feature between the spectra of both these compounds lies within the fingerprint region of 500 to 400 cm^{-1} .

Predictive Model

According to our spectrophotometric analysis, plasma choline and TMAO levels were significantly altered in control/CAD patients. We intended to determine the potential utility of circulating TMAO levels as a diagnostic biomarker of CAD. Hence, ROC analysis was performed to evaluate the predictive power considering the age, sex, and history of diabetes, serum choline, and TMAO concentrations as contributing parameters to CAD. The obtained ROC graph (Figure 6) has an area under the curve (AUC) = 0.893.

Table 1. Patient Clinical History

Patient Number	Presence of CAD	Choline Concentration in μM	TMAO Concentration in μM	Significant History
P1	CAD	42.81313632	0.721847931	Diabetes, smoking
P2	CAD	31.32668511	1.328200192	Akinetic
P3	CAD	48.03425051	2.204042348	-

Patient Number	Presence of CAD	Choline Concentration in μM	TMAO Concentration in μM	Significant History
P4	CAD	56.38803321	1.732435034	-
P5	CAD	33.93724221	1.530317613	Surgery
P6	CAD	38.11413356	1.790182868	High BP
P7	CAD	43.85735916	2.001924928	-
P8	CAD	58.47647888	2.011549567	Heavy smoker, FBS, hypokinetic myocardium
P9	CAD	35.50357646	2.098171319	Rheumatoid, akinetic
P10	CAD	33.41513079	2.550529355	High BP, Hypertension, diabetes
P11	CAD	190.5706678	2.155919153	Stent, high BP, diabetes, Overweight
P12	CAD	195.791782	2.069297401	6 stents, High BP, diabetes
P13	CAD	142.0143059	2.598652551	Smoker, osteoarthritis
P14	CAD	34.98146504	0.529355149	High BP, stent
C1	No CAD	110.1655093	0.250240616	-
C2	No CAD	37.59202214	0.028873917	-
C3	No CAD	69.96293009	0.51973051	Arteriosus
C4	No CAD	17.22967681	1.164581328	Neurological condition
C5	No CAD	46.46791625	1.828681424	Diabetes
C6	No CAD	2.610557093	1.405197305	Diabetes, smoking

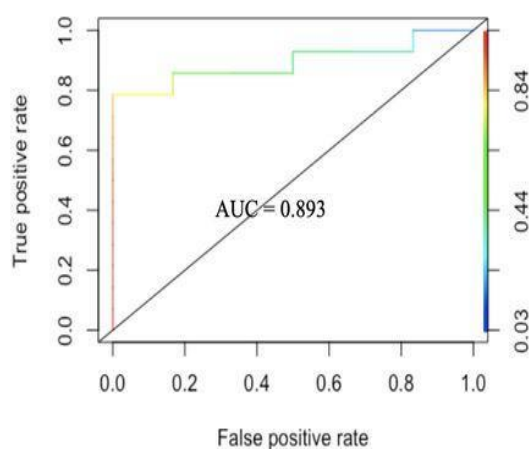


Figure 6. Receiver Operator Characteristics Graph

We formed a multivariate regression model to calculate the odds of having CAD using these parameters. The results are summarized in [Table 2](#).

Table 2. Results of Multivariate Logistic Regression in R.

Coefficients	Estimate	Std. Error	Z value	Pr (> Z)
(Intercept)	-4.85989	3.53618	-1.374	0.1693
TMAO concentration	2.80055	1.40663	1.991	0.0465
Age	0.01232	0.03557	0.346	0.7291
Sex	1.69448	1.74369	0.972	0.3312
Diabetes	-1.91948	1.65473	-1.160	0.2461
Choline concentration	0.02248	0.02508	0.896	0.3701

TMAO concentration was identified to be a significant and powerful predictor for CAD diagnosis, as evidenced by its low p-value ($P < 0.05$). Hence, we considered these parameters to form a preliminary multivariate logistic regression equation.

$$f(x) = -4.859 + 2.8*(\text{TMAO Concentration}) + 0.012*(\text{Age}) + 1.69*(\text{Male}) - 1.919*(\text{Diabetes}) + 0.02*(\text{Choline Concentration})$$

Where $f(x)$ is the log (odds of having CAD).

To calculate P, the odds of having CAD, we use the formula:

$$P = \exp(f(x)) / (1 + \exp(f(x)))$$

If $P \geq \text{cut-off} = 0.795$, then the person can be considered as a CAD patient.

4. Discussion

Although there is enough evidence of the contribution of gut-derived metabolite TMAO in the progression of cardiometabolic disorders, studies characterizing gut bacteria responsible for the production of TMAO in CAD patients are lacking. Growth rate becomes an essential factor to consider while trying to identify the effect of a particular environmental condition on bacterial growth (8). In particular, a higher growth rate implies faster bacterial growth and generation time. The influence of incubation time for the completion of each growth cycle was determined to be between 22 and 24 hours. For *P. vulgaris*, we observe the highest growth rate at the 8.5 pH state, followed by 9, 7.4, and 6.4, respectively. For *P. mirabilis*, we observe the highest growth rate at the 7.4 pH state, followed by 8.5, 9, and 6.4, respectively. Correlating these pH states to that found within the different compartments of the GI tract of the human body, we may infer that the local micro-environment conditions of the intestines, with their neutral to alkaline pH, optimally support the growth of *P. vulgaris* and *P. mirabilis*. From the saturation curves, it was observed that at pH 9 in *P. vulgaris*, 45% of salt concentration gives the highest protein yield. At pH 8.5 in *P. mirabilis*, 45% of salt concentration gives the highest yield of protein. Of salt concentration, 45% can be taken as the optimal concentration for the organism and pH state, respectively.

The present study is the first of its kind in that it provides new information about the relation between plasma levels of TMAO and CAD in Indian patients. Other investigative studies have reported the median choline and TMAO concentrations in CAD patients to be 41.1 μM and 3.7 μM , respectively (21). We

hypothesize that this difference could be due to considering a different cohort. Therefore factors like diet, lifestyle, and health conditions can contribute to the observed differences in serum choline levels.

Table 1 summarises the clinical histories of the patients included in this study. Our serum metabolite quantification results correlate with the patients' clinical histories. P9 has a history of rheumatoid arthritis (RA). According to our observations, this patient has low choline and high TMAO levels in her serum. Low serum choline levels are associated with RA due to higher uptake and metabolism by the inflamed tissues (21). Therefore, in addition to higher consumption by the gut bacteria, this clinical history could also account for the decrease in circulating free choline in the patient.

Furthermore, RA and CVDs have been found to be interrelated by the associated inflammation (which is a characteristic of RA) (22). This inflammation leads to stress, which activates the inflammasome, ultimately promoting the formation of atherosclerotic lesions. TMAO, a metabolite associated with promoting these inflammation factors, is present in high concentrations in such conditions. This could be an explanation for the high serum TMAO concentration detected. P11 and P12 both have histories of type II diabetes and stent usage. These patients demonstrate high choline and TMAO concentrations in their serum. High serum choline concentrations have been found to be associated with increased T2DM risk (23). The association between high TMAO levels and T2DM patients has also been well documented (24, 25). Our results fall in line with these findings. P13 has a history of osteoarthritis. Some studies have identified risk factors such as aging, obesity, and chronic inflammation being common between CVD and osteoarthritis (26). Thus, high choline levels could be derived from sources other than the diet, for example, mechanisms like platelet rupture and increased leukocyte-PLD activity in inflammation, to name a few (27). TMAO has been identified as a potential player in the inflammatory phenotype associated with arthritis (28). This could support the high TMAO concentration in this patient's serum.

Additionally, our study demanded a test to allow the qualitative analysis of the metabolites. To meet this purpose, Trotter *et al.*'s (2016) study used FTIR spectroscopy to analyze the functional groups of compounds. On applying the same technique, we arrive at the spectra of choline and TMAO that show a very strong and broad band at 3348.18 cm^{-1} , which is assigned to -OH stretching vibration. The shape of the band most likely indicates the presence of intramolecular hydrogen bonds since choline posse-

sses both hydrogen bonding donors and acceptors. The weak peak at 2165.15 cm^{-1} confirms the presence of hydrogen bonds (29), and the sharp peak at 1635.52 cm^{-1} corresponds to the deformation vibration of NH_3^+ . These bands characterize the functional groups present in both compounds. On comparing the spectral results of the serum samples with that of the standards, we see that the bands are similar to that obtained in the standard spectra. Therefore, it can be concluded that the test confirms the presence of choline and TMAO in the serum samples.

Several studies have focused on statistical analysis to determine the utility of modifiable risk factors to improve the clinical prognosis of CAD progression. Here, we aimed to develop a preliminary predictive model for CAD diagnosis using 5 known risk factors amongst a sample size of 20 individuals. This model can be considered as a building block, which, when expanded to include larger sample sizes, categories, and statistical analyses, becomes an accurate and practical CAD diagnostic tool for medical practitioners.

ROC analysis and the subsequent logistic regression model revealed circulating TMAO levels' predictive power in our study. We observe that the ROC graph is skewed towards the true positive rate. Taken together, this indicates that the selected parameters of age, sex, history of diabetes, choline, and TMAO serum concentrations are good predictors of CAD. The cut-off value was selected as 0.795. This is the value where the true positive rate is high along with a significantly low false positive rate, which is a desirable characteristic of a diagnostic equation or tool. Multivariate logistic regression analysis further revealed the strong association of TMAO expression with CAD. While our model does not indicate any other parameters to be significant, possibly due to the small sample size, it has already been well documented in the literature that age, diet, sex, and history of diabetes are essential contributors to the development and progression of CAD (24, 30, 31, 32). In fact, evidence produced by several scholars across the globe has stressed the need to practice a well-tested healthy dietary pattern. This pattern emphasizes plant protein sources and reduced animal fat intakes to reduce CVD. An Asian diet with the lowest meat intake and highest legume consumption puts Indians in the low-risk category for developing comorbidities.

In all, further research on the gut microbiome as an ecosystem is necessary towards understanding the

Proteus species in terms of its role in disease and interactions with other gut microbes. This data could help identify the risks imparted by the gut microbiota in CAD and help devise appropriate medications. For example, identifying gut microbiota targeting antibiotics and Choline TMA Lyase inhibitors as CAD therapeutics could be an exciting study area.

5. Conclusion

Choline TMA Lyase functionality is optimal at the neutral and alkaline pH range, as found in the small and large intestines. Our findings demonstrate the optimum bacterial growth for *P. mirabilis* and *P. vulgaris* within the same range of 7.4-9.0. Taken together, these results point towards the strong pathological potential of *Proteus* bacteria in the progression of CAD. This introduces *Proteus* bacteria as a new potential therapeutic target for CAD. The results of quantitative estimation by spectrophotometry identified TMAO to be a significant and powerful predictor for CAD in Indian patients. While the general trend observed was that CAD patients had low serum choline and high serum TMAO concentrations, patients with significant clinical conditions like diabetes and arthritis had high serum choline and TMAO concentrations. Finally, the proposed predictive model template, once improved upon by taking a larger sample size and expanding the parameters to include detailed categories, could serve as a useful tool for the progressive assessment of the risk factors for CAD by medical practitioners.

Acknowledgment

We would like to thank Dr. Shekhar Rao, Director, Sri Sathya Sai Institute of Higher Medical studies and Hospital, Whitefield, Bangalore, for providing us with patient's sample. Dr. Anjana Gopi, Head of the department of Microbiology, KIIMS, Bangalore, for providing us with microbial cultures.

Funding

None.

Conflict of Interest

The authors declare any conflict of interest.

Reference

- Kazemian N, Mahmoudi M, Halperin F, Wu JC, Pakpour S. Gut microbiota and cardiovascular disease: opportunities and challenges. *Microbiome*. 2020;8(1):1-7. [PMID] [PMCID] [DOI:10.1186/s40168-020-00821-0]
- Dalla Via A, Gargari G, Taverniti V, Rondini G, Velardi I, Gambaro V, et al. Urinary TMAO levels are associated with the taxonomic composition of the gut microbiota and with the choline TMA-lyase gene (cutC) harbored by Enterobacteriaceae. *Nutrients*. 2020;12(1):62. [DOI:10.3390/nu12010062] [PMID] [PMCID]
- Jonsson AL, Bäckhed F. Role of gut microbiota in atherosclerosis. *Nat Rev Cardiol*. 2017;14(2):79-87. [DOI:10.1038/nrcardio.2016.183] [PMID]
- Wang Z, Klipfell E, Bennett BJ, Koeth R, Levison BS, DuGar B et al. Gut flora metabolism of phosphatidylcholine promotes cardiovascular disease. *Nature*. 2011 Apr;472(7341):57-63. [DOI:10.1038/nature09922] [PMID] [PMCID]
- Zhu Y, Li Q, Jiang H. Gut microbiota in atherosclerosis: focus on trimethylamine N-oxide. *APMIS*. 2020;128(5):353-66. [DOI:10.1111/apm.13038] [PMID] [PMCID]
- Jin M, Qian Z, Yin J, Xu W, Zhou X. The role of intestinal microbiota in cardiovascular disease. *J Cell. Mol. Med*. 2019 Apr;23(4):2343-50. [DOI:10.1111/jcmm.14195] [PMID] [PMCID]
- Mobley HL, Belas R. Swarming and pathogenicity of *Proteus mirabilis* in the urinary tract. *Trends Microbiol*. 1995;3(7):280-4. [DOI:10.1016/S0966-842X(00)88945-3]
- Hamilton AL, Kamm MA, Ng SC, Morrison M. *Proteus* spp. as putative gastrointestinal pathogens. *Clin Microbiol Rev*. 2018;31(3):e00085-17. [DOI:10.1128/CMR.00085-17] [PMID] [PMCID]
- Jameson E, Fu T, Brown IR, Paszkiewicz K, Purdy KJ, Frank S, Chen Y. Anaerobic choline metabolism in microcompartments promotes growth and swarming of *Proteus mirabilis*. *Environ Microbiol*. 2016;18(9):2886-98. [DOI:10.1111/1462-2920.13059] [PMID] [PMCID]
- Schaffer JN, Pearson MM. *Proteus mirabilis* and urinary tract infections. *Microbiol Spectr*. 2015; 3(5):0017-2013. [DOI:10.1128/microbiolspec.UTI-0017-2013] [PMID] [PMCID]
- Yatsunenکو T, Rey FE, Manary MJ, Trehan I, Dominguez-Bello MG, Contreras M, et al. Human gut microbiome viewed across age and geography. *Nature*. 2012 Jun;486(7402):222-7. [DOI:10.1038/nature11053] [PMID] [PMCID]
- Bergey, D. H., Noel R. Krieg, and John G. Holt. *Bergey's Manual of Systematic Bacteriology*. Baltimore, MD: Williams & Wilkins, 1984.
- Berg JM, Tymoczko JL, Stryer L. *Biochemistry*. 5th edition. New York: W H Freeman; 2002.
- Lowry OH, Rosebrough NJ, Farr AL, Randall RJ. Protein measurement with the Folin phenol reagent. *J Biol Chem*. 1951;193:265-75. [DOI:10.1016/S0021-9258(19)52451-6]
- Al-Tubuly AA. SDS-PAGE and western blotting. In *Diagnostic and Therapeutic Antibodies 2000* (pp. 391-405). Humana, Totowa, NJ. [DOI:10.1385/1-59259-076-4:391] [PMID]
- Appleton HD, La Du BN, Levy BB, Steele JM, Brodie BB. A chemical method for the determination of free choline in plasma. *J Biol Chem*. 1953;205(2):803-13. [DOI:10.1016/S0021-9258(18)49224-1]
- Wang Z, Tang WW, Buffa JA, Fu X, Britt EB, Koeth RA, Levison BS, Fan Y, Wu Y, Hazen SL. Prognostic value of choline and betaine depends on intestinal microbiota-generated metabolite trimethylamine-N-oxide. *Eur Heart J*. 2014;35(14):904-10. [DOI:10.1093/eurheartj/ehu002] [PMID] [PMCID]
- Wekell JC, Barnett H. New method for analysis of trimethylamine oxide using ferrous sulfate and EDTA. *J Food Sci*. 1991;56(1):132-5. [DOI:10.1111/j.1365-2621.1991.tb07993.x]
- Moraes LG, Rocha RS, Menegazzo LM, Araújo EB, Yukimito K, Moraes JC. Infrared spectroscopy: a tool for determination of the degree of conversion in dental composites. *J Appl Oral Sci*. 2008;16:145-9. [DOI:10.1590/S1678-77572008000200012] [PMID] [PMCID]
- Kalnins G, Kuka J, Grinberga S, Makrecka-Kuka M, Liepinsh E, Dambrova M et al. Structure and function of CutC choline lyase from human microbiota bacterium *Klebsiella pneumoniae*. *J Biol Chem*. 2015;290(35):21732-40. [DOI:10.1074/jbc.M115.670471] [PMID] [PMCID]
- Cedola F, Coras R, Sanchez-Lopez E, Mateo L, Pedersen A, Brandy-Garcia A. et al. Choline metabolite is associated with inflammation in arthritis in the elderly. *Arthritis Rheumatol*. 2019 Oct 1 (Vol. 71). 111 RIVER ST, HOBOKEN 07030-5774, NJ USA: WILEY.
- Chan MM, Yang X, Wang H, Saaoud F, Sun Y, Fong D. The microbial metabolite trimethylamine N-

- oxide links vascular dysfunctions and the autoimmune disease rheumatoid arthritis. *Nutrients*. 2019;11(8):1821. [DOI:10.3390/nu11081821] [PMID] [PMCID]
23. Mazidi M, Katsiki N, Mikhailidis DP, Banach M. Dietary choline is positively related to overall and cause-specific mortality: results from individuals of the National Health and Nutrition Examination Survey and pooling prospective data. *Br J Nutr*. 2019;122(11):1262-70. [DOI:10.1017/S0007114519001065] [PMID]
24. Dambrova M, Latkovskis G, Kuka J, Strele I, Konrade I, Grinberga S et al. Diabetes is associated with higher trimethylamine N-oxide plasma levels. *Exp Clin Endocrinol. Diabetes*. 2016;124(04):251-6. [DOI:10.1055/s-0035-1569330] [PMID]
25. Dong Z, Liang Z, Guo M, Hu S, Shen Z, Hai X. The association between plasma levels of trimethylamine N-oxide and the risk of coronary heart disease in Chinese patients with or without type 2 diabetes mellitus. *Dis Markers*. 2018;2018. [DOI:10.1155/2018/1578320] [PMID] [PMCID]
26. Liu W, Balu N, Canton G, Hippe DS, Watase H, Waterton JC et al. Understanding atherosclerosis through an osteoarthritis data set: From knee to vessel. *Arterioscler Thromb Vasc Biol*. 2019;39(6):1018-25. [PMID] [PMCID] [DOI:10.1161/ATVBAHA.119.312513]
27. Danne O, Möckel M. Choline in acute coronary syndrome: an emerging biomarker with implications for the integrated assessment of plaque vulnerability. *Exp Rev Mol Diagn*. 2010 Mar 1;10(2):159-71. [DOI:10.1586/erm.10.2] [PMID]
28. Coras R, Kavanaugh A, Boyd T, Huynh D, Lagerborg KA, Xu YJ et al. Choline metabolite, trimethylamine N-oxide (TMAO), is associated with inflammation in psoriatic arthritis. *Clin Exp Rheumatol*. 2019;37(3):481.
29. Wang H, Jia Y, Wang X, Ma J, Jing Y. Physico-chemical Properties of Magnesium Ionic Liquid Analogous. *J Chil Chem*. 2012;57(3):1208-12. [DOI:10.4067/S0717-97072012000300003]
30. Witkowski M, Weeks TL, Hazen SL. Gut microbiota and cardiovascular disease. *Circ Res*. 2020;127(4):553-70. [DOI:10.1161/CIRCRESAHA.120.316242] [PMID] [PMCID]
31. Xu H, Duan Z, Miao C, Geng S, Jin Y. Development of a diagnosis model for coronary artery disease. *Indian Heart J*. 2017;69(5):634-9. [DOI:10.1016/j.ihj.2017.02.022] [PMID] [PMCID]
32. Bishnoi S, Kaushik RM, Rawat A, Dhar M, Kaushik R. Risk factors for angiographically proven coronary artery disease in women in India. *Health Care Women Int*. 2016;37(12):1357-72. [DOI:10.1080/07399332.2016.1215463] [PMID]